Dosimetric characteristics of a newly designed grid block for megavoltage photon radiation and its therapeutic advantage using a linear quadratic model

Ali S. Meigooni,[a] Kai Dou, Navid J. Meigooni, Michael Gnaster, Shahid Awan, Sharifeh Dini, and Ellis L. Johnson
University of Kentucky Chandler Medical Center, Department of Radiation Medicine, Lexington, Kentucky 40536-0084

(Received 7 March 2006; revised 29 June 2006; accepted for publication 6 July 2006; published 17 August 2006)

Grid radiation therapy with megavoltage x-ray beam has been proven to be an effective technique for management of large, bulky malignant tumors. The clinical advantage of GRID therapy, combined with conventional radiation therapy, has been demonstrated using a prototype GRID block [Mohiuddin, Curtis, Grizos, and Komarnicky, Cancer **66**, 114–118 (1990)]. Recently, a new GRID block design with improved dosimetric properties has become commercially available from Radiation Product Design, Inc. (Albertive, MN). This GRID collimator consists of an array of focused apertures in a cerrobend block arranged in a hexagonal pattern having a circular cross-section with a diameter and center-to-center spacing of 14.3 and 21.1 mm, respectively, in the plane of isocenter. In this project, dosimetric characteristics of the newly redesigned GRID block have been investigated for a Varian 21EX linear accelerator (Varian Associates, Palo Alto, CA). These determinations were performed using radiographic films, thermoluminescent dosimeters in Solid Water™ phantom materials, and an ionization chamber in water. The output factor, percentage depth dose, beam profiles, and isodose distributions of the GRID radiation as a function of field size and beam energy have been measured using both 6 and 18 MV x-ray beams. In addition, the therapeutic advantage obtained from this treatment modality with the new GRID block design for a high, single fraction of dose has been calculated using the linear quadratic model with α/β ratios for typical tumor and normal cells. These biological characteristics of the new GRID block design will also be presented.
[DOI: 10.1118/1.2241998]

Key words: grid therapy, megavoltage photon radiation, dosimetry, cell survival, therapeutic advantage

I. INTRODUCTION

Megavoltage GRID radiation therapy is a new paradigm in the management of bulky (>8 cm) malignant tumors.[1–4] The Department of Radiation Medicine at the University of Kentucky has utilized a modified spatially fractionated technique with megavoltage x-ray beam for treatment of advanced tumors.[3,4] Dosimetric characteristics of these GRID radiation fields for both photon and electron beams have been studied by several investigators.[5–7] It is interesting to know that the published clinical results[1–4] were obtained with a prototype GRID block that was constructed by placing several segments of copper tubing between two plastic trays and filling the space between the tubes with cerrobend material. Therefore, the differences in attenuation between the copper tubing and cerrobend material, as well as the nondivergent match problem of the copper tubing to the divergent beam, brought about a challenge to the design of the prototype GRID block. Despite the problems mentioned above in the prototype GRID block design, Mohiuddin *et al.*[3] have shown that the overall response rate of patients increased from 62% to 91% when they were treated with a single-field GRID irradiation of ⩾15 Gy plus conventional external beam therapy.

Recently, a new GRID block has been designed and fabricated by Radiation Product Design, Inc. (5218 Barthel Industrial Dr., Albertive, MN). This block was constructed by casting the divergent holes in a cerrobend block, using a stereotactic method which is able to provide the optimal conditions of: (1) accurate beam divergence and (2) less transmission through the blocked area. This block design allows for a greater volume of tissue to receive the therapeutic dose of greater than 85%. The hole size and center-to-center spacing can be customized, and also the divergence of the holes can be designed to match one of the commercially available linear accelerators. Characterization of the dosimetric and biological properties of the new GRID block design is necessary for clinical implementation.

While the evaluation of dosimetric properties of GRID irradiation is relatively straightforward, the biological analysis is much more difficult. The radiobiology of GRID irradiation is not well understood and is currently being studied by several investigators.[8,9] Proposed mechanisms of action include the production of various cytokines in the irradiated tissues.[9] For a nonuniform radiation field, Niemierko[10] introduced a radiobiological model, based on the linear quadratic model, to describe the biological effectiveness of the inho-

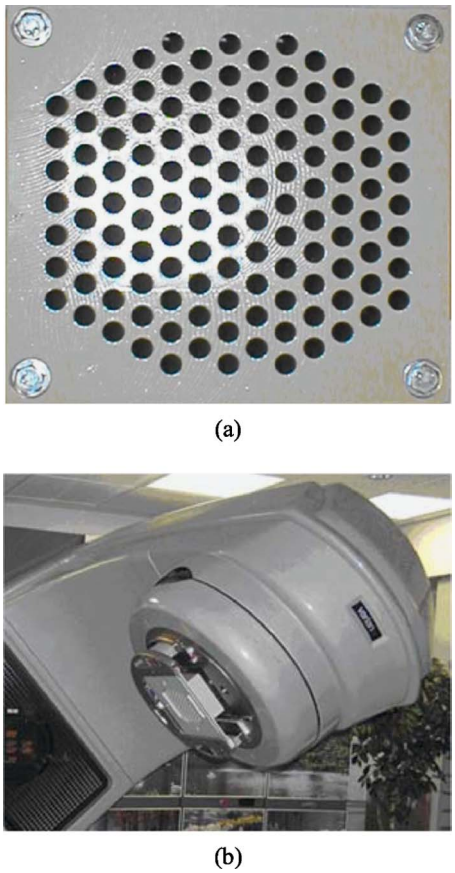

FIG. 1. (a) Top view of a newly designed GRID block. (b) Photograph of the GRID block mounted on a Clinac 21EX linear accelerator.

mogeneous dose distribution such as three-dimensional (3D) conformal therapy. Zwicker *et al.*[11] have extended this model to evaluate radiobiological properties of GRID irradiation. They have concluded that for a wide range of tumor tissue sensitivities, a single-dose partial-volume GRID radiation field may have a significant therapeutic advantage over open field radiotherapy in sparing normal tissues.

The goal of this project is to investigate the physical and biological characteristics of the megavoltage photon radiation through this newly designed GRID block for a Varian 21EX linear accelerator (Varian Associates, Palo Alto, CA). Dosimetric characteristics [i.e., beam profiles, isodose distributions, output factor, and percent depth dose (%DD) of radiation field] for this block design were experimentally determined. Measurements were performed for 6 and 18 MV x-ray beams using radiographic film and thermoluminescent dosimeters (TLDs) in Solid Water™ phantom material (Radiation Measurements Inc., RMI, Middleton, WI) and an ionization chamber in water. The biological analysis of the new GRID block utilizes the above mentioned model by Zwicker *et al.*[11]

II. MATERIALS AND METHODS

A. Grid design

The GRID block used in the current experiment was manufactured by Radiation Products Design, Inc. This block

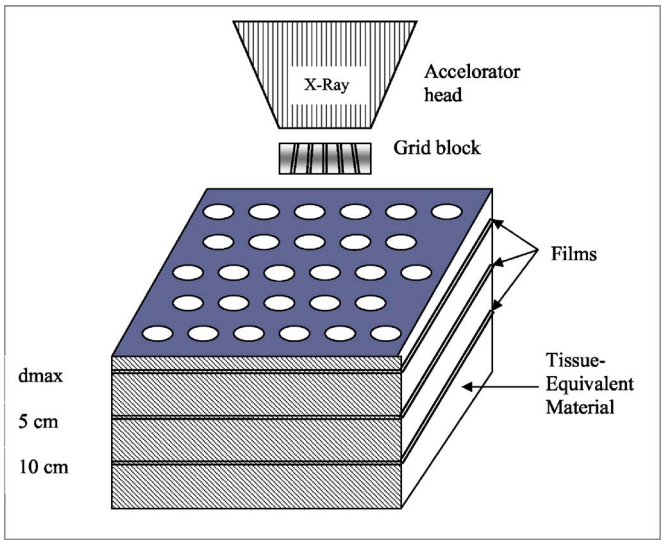

FIG. 2. Schematic diagram of the experimental setup for film dosimetry using 6 and 18 MV photon GRID fields.

was constructed by casting a hexagonal array of divergent holes 14.3 mm in diameter with 21.1 mm center-to-center spacing projected in the plane of isocenter. The apertures were cast in a 7.5-cm-thick cerrobend block. The divergence of the holes was designed for a Varian 21EX linear accelerator having a source-to-tray distance of 65.4 cm. Similar to the prototype GRID block, the new GRID aperture design provides approximately 41.7% open area at isocenter. Various field sizes up to a maximum of 25×25 cm can be achieved with this block design. Figure 1(a) shows the top view of the GRID block. Figure 1(b) illustrates the GRID block mounted in the block tray holder of the Varian 21EX linear accelerator.

B. Film dosimetry

Film dosimetry was utilized to obtain beam profiles for the GRID collimated fields using 6 and 18 MV photon

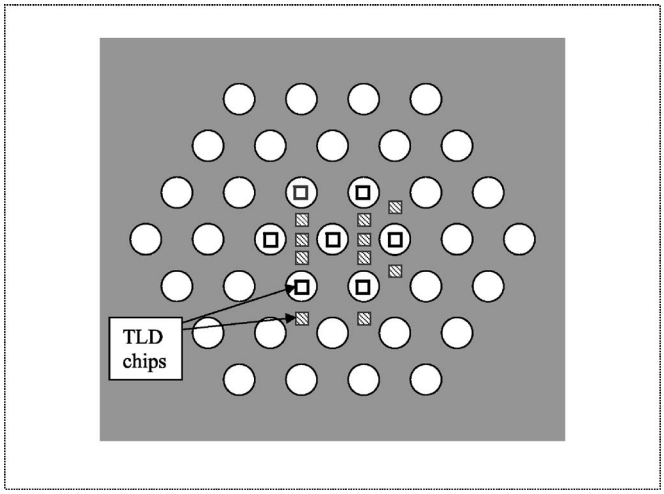

FIG. 3. Schematic diagram of the experimental setup for TLD (square symbol) dosimetry in a GRID radiation field.

TABLE I. (A) Dose rates (cGy/MU) of 6 MV x-ray beam for a newly designed GRID block as a function of depth measured with TLD and film in Solid Water™ and an ionization chamber in water for a 10×10 cm field. (B) Dose rates (cGy/MU) of 18 MV x-ray beam for a newly designed GRID block as a function of depth measured with TLD and film in Solid Water™ and an ionization chamber in water for 10×10 cm field.

			Dose rate (cGy/MU)		Relative dose rate (%)
	Methods	Depth (cm)	Open area	Blocked area	Blocked-to-open area
(A)	TLD	1.5	0.89	0.12	13.5
		5.0	0.70	0.11	15.7
		10.0	0.55	0.11	20.0
	Film	1.5	0.87	0.11	12.6
		5.0	0.70	0.12	17.1
		10.0	0.55	0.11	20.0
	Ionization chamber	1.5	0.89	0.12	13.5
		5.0	0.73	0.11	15.1
		10.0	0.54	0.10	18.5
(B)	TLD	2.5	0.78	0.17	21.8
		5.0	0.73	0.18	24.7
		10.0	0.56	0.18	32.1
	Film	2.5	0.78	0.15	19.2
		5.0	0.69	0.15	21.7
		10.0	0.57	0.14	24.6
	Ionization chamber	2.5	0.78	0.20	25.6
		5.0	0.73	0.20	27.4
		10.0	0.58	0.17	29.3

beams from a Varian Clinac 21EX linear accelerator. The measurements were performed in Solid Water™ phantom materials using Kodak X-Omat V radiographic film (Eastman Kodak Company, Rochester, NY). The beam profiles were measured along the two orthogonal directions (in plane and cross plane) in a plane perpendicular to the central beam axis. These measurements were performed at depths of dmax, 5 cm, and 10 cm in 23-cm-thick Solid Water™ phantom material for 6 and 18 MV x-ray beams (Fig. 2). The irradiated films were read with a Lumiscan-50 laser scanner (Lumisys, Sunnyvale, CA) and processed with MEPHYSTO software (Version 6.30, PTW-New York Co., Hicksville, New York), Microsoft Excel, and Origin® Version 6.1 (OriginLAB Corp, One Roundhouse Plaza, Northampton, MA). Batch- and energy-specific calibration curves were used to obtain doses for the measured transmittance. Calibrations were obtained for doses of 1, 5, 10, 20, 30, 50, 60, and 70 cGy using a 10×10 cm open field at 100 cm SSD at depth of dmax in Solid Water™ phantom material.

C. TLD technique and phantom design

TLD measurements were performed at depths of dmax, 5 cm, and 10 cm for both 6 and 18 MV x-ray beams using LiF TLD chips (TLD-100, Thermo Electron Corp., Oakwood Village, OH) in Solid Water™ phantom material. This phantom material was accurately machined to accommodate the $1\times1\times1$ mm^3 TLD chips at the center of the GRID holes and blocked areas (Fig. 3). The irradiated TLD response was obtained using a Harshaw Model 3500 TLD reader (Thermo Electron Corp., Oakwood Village, OH). The responses of at least 10 TLD chips, from the same batch of TLDs, were calibrated using open radiation field (i.e., 10×10 cm^2) with 6 MV x-ray beams. The corresponding responses from the TLDs irradiated in the GRID field were then converted to dose following procedures described by Meigooni *et al.*[12] The mean values of up to seven chips were used to evaluate each measurement point.

Application of TLD chips for radiation dosimetry in both external beam and brachytherapy fields have been demonstrated by various investigators.[12–16] Equation (1) was used to calculate the absorbed dose rate from the TLD responses for each point irradiated in the phantom:[12]

$$\dot{D}(d)=\frac{R(d)}{MU\,.\,\varepsilon\,.\,F_{\mathrm{lin}}}, \tag{1}$$

where $\dot{D}(d)$ is the absorbed dose per monitor unit (MU) at depth of d, R is the TLD response corrected for background and the physical differences between the TLD chips using predetermined chip factors, MU is the monitor unit used for the exposure of TLDs, ε is the calibration factor for the TLD response (nC/cGy) measured with a 6- or 18-MV x-ray beam from a linear accelerator, and F_{lin} is the nonlinearity

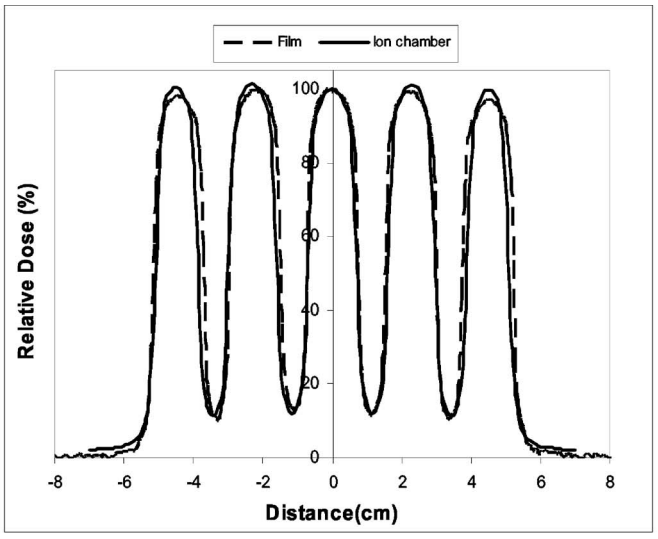

FIG. 4. Comparison of beam profiles for 6 MV x ray obtained using film and ionization chamber dosimetry at depths of (a) 1.5 and (b) 10 cm.

correction of the TLD response for the given dose. In these measurements, the absorbed dose exposure level was selected to be in the range of 10–100 cGy for which F_{lin} was assumed to be unity.[12]

D. Ion chamber measurements

Percent depth dose and beam profiles were measured using a Scanditronix Wellhofer 3D radiation scanning system (Scanditronix Wellhofer North America, Bartlett, TN) with a Wellhofer Model CC01 chamber. This microchamber has a sensitive volume of 0.01 cm^3 (1 mm radius and 3.6 mm active length). The chamber was scanned in the direction of the chamber diameter, which provides a sufficiently small spatial resolution, relative to the GRID hole diameter (14 mm), for dosimetry of GRID radiation field. These measurements were performed as a function of depth, field size, and beam energy. This system consisted of a standard $48\times48\times48$ cm^3 water tank, Wellhofer Model CU 500E dual channel control unit, and WP 700 software. For output factor measurements, the CC01 ionization chamber charge readings were obtained with an Inovision Model 35040 electrometer. Output factors were then obtained by calculating the ratio of the average charge readings for a 10×10 cm field without to with GRID block at dmax depth and 100 cm SSD.

TABLE II. Output factors as a function of field size and energy of the newly designed GRID block measured at dmax (1.5 cm for 6 MV and 2.5 cm for 18 MV) and 100 cm SSD with an ionization chamber in water as a function of field size and energy.

	Output factor (cGy/MU)				
	5×5	10×10	15×15	20×20	25×25
6 MV	0.88	0.89	0.91	0.92	0.93
18 MV	0.75	0.78	0.81	0.83	0.84

E. Therapeutic advantage of GRID therapy

The methodology of Zwicker *et al.*[11] has been used to evaluate the potential therapeutic advantage of the newly designed GRID field. The overall survival fraction (SF) is determined from an area weighted average of local SF and is calculated for both normal and tumor cells. Uniform field calculations are also performed for a dose level that gives the same tumor SF in both the open and GRID fields. The therapeutic advantage is then defined as

$$\text{Therapeutic Advantage} = \frac{SF_{\text{GRID field}}^{\text{Normal tissue}}}{SF_{\text{Open field}}^{\text{Normal tissue}}}, \tag{2}$$

where each normal-tissue SF is calculated for the same tumor SF. The α/β ratios used for these calculations, 10 Gy for tumor cells and 2.5 Gy for normal cells, represent typical values for these tissue types.

III. RESULTS AND DISCUSSION

A. Dosimetric characteristics

To validate the use of different dosimeters in this investigation, the results obtained using TLD, ionization chamber, and film dosimetry were compared in graphical and tabulated formats. Tables I(A) and I(B)show excellent agreement ($\pm5\%$) among the three techniques in measuring the output factors for both 6 and 18 MV x-ray beams, respectively. Figures 4(a) and 4(b) show the excellent agreement between the dose profiles of 6 MV x rays measured with the film dosimetry technique and those measured with ionization chamber, at dmax and 10 cm depths. Similar results were obtained for 18 MV photon beams. With these validations, any of these dosimetric techniques could be utilized for the remainder of these investigations. The output factors of the new GRID block as a function of field size for both 6 and 18 MV were measured in water using the ionization chamber (Table II). The open field $S_{c,p}$ was compared with GRID relative outputs

TABLE III. Comparison of open field $S_{c,p}$ with GRID relative outputs at dmax and 100 cm SSD as a function of field size and energy.

		Field size (cm^2)				
		5×5	10×10	15×15	20×20	25×25
6 MV	Relative output factor	0.984	1.000	1.017	1.030	1.038
	$S_{c,p}$	0.940	1.000	1.034	1.059	1.073
18 MV	Relative output factor	0.960	1.000	1.032	1.054	1.070
	$S_{c,p}$	0.921	1.000	1.041	1.065	1.078

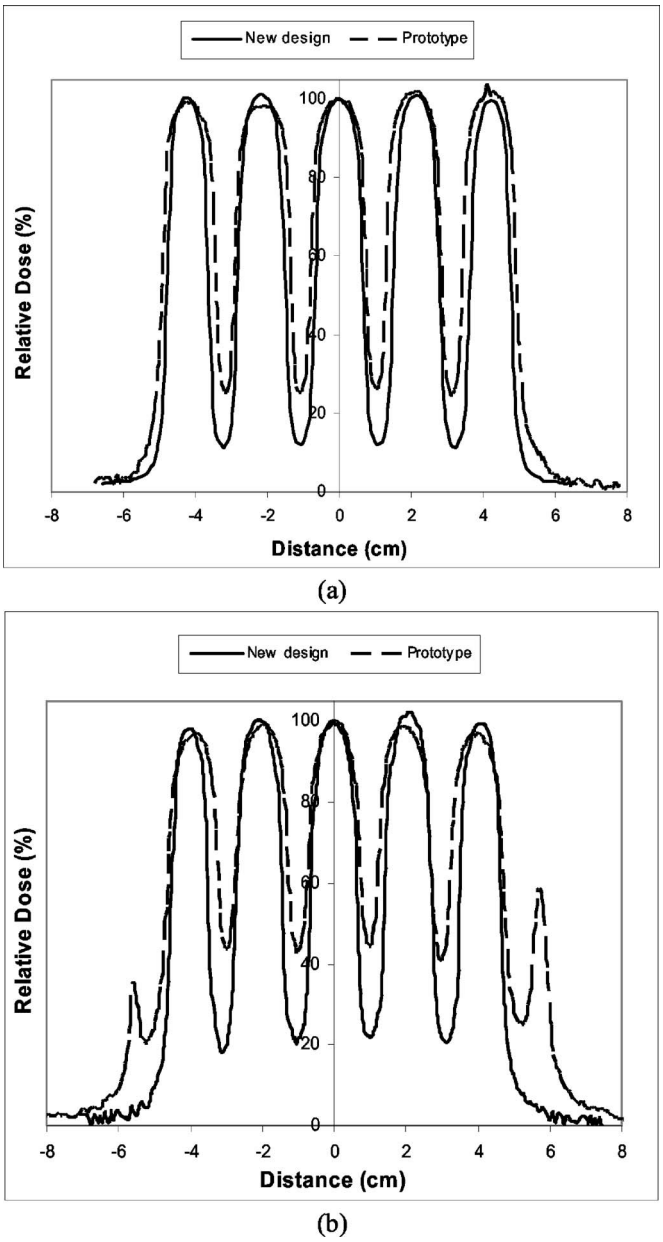

FIG. 5. Comparison of transverse profiles from film dosimetry for newly designed and prototype GRID for a 10×10 cm field at the depth of maximum dose in Solid Water™ phantom material using (a) 6 and (b) 18 MV x-ray irradiation.

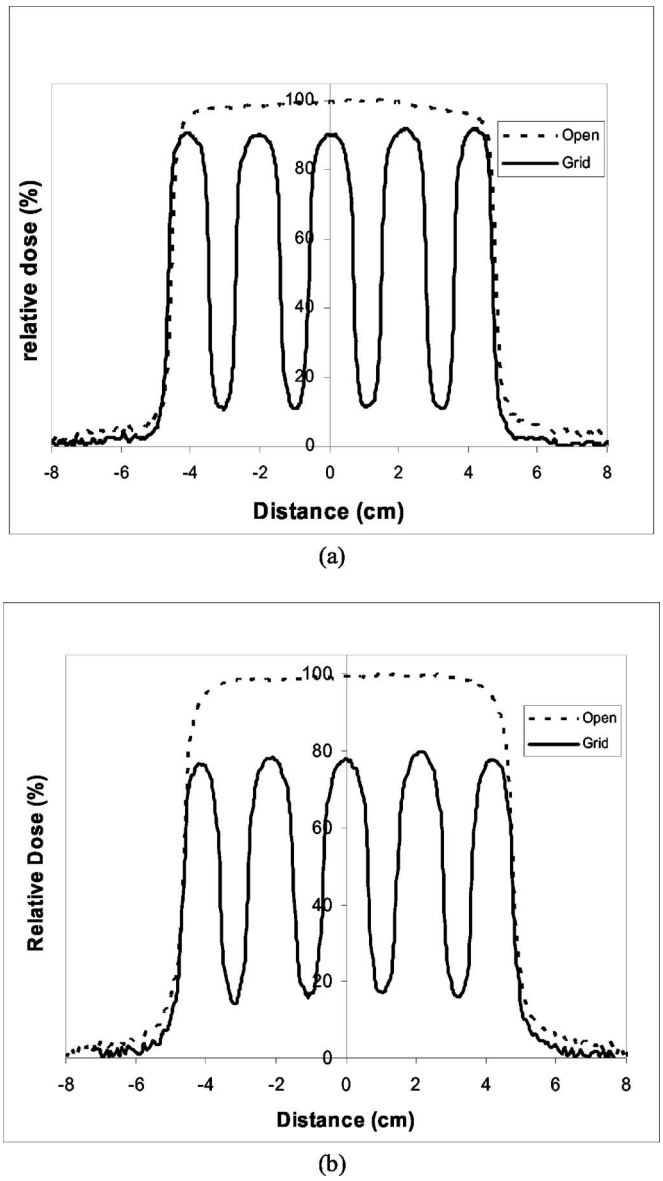

FIG. 6. Comparison of transverse profiles from film dosimetry for an open field and a GRID field for a 10×10 cm field at the depth of maximum dose in Solid Water™ phantom material using (a) 6 and (b) 18 MV x-ray irradiation.

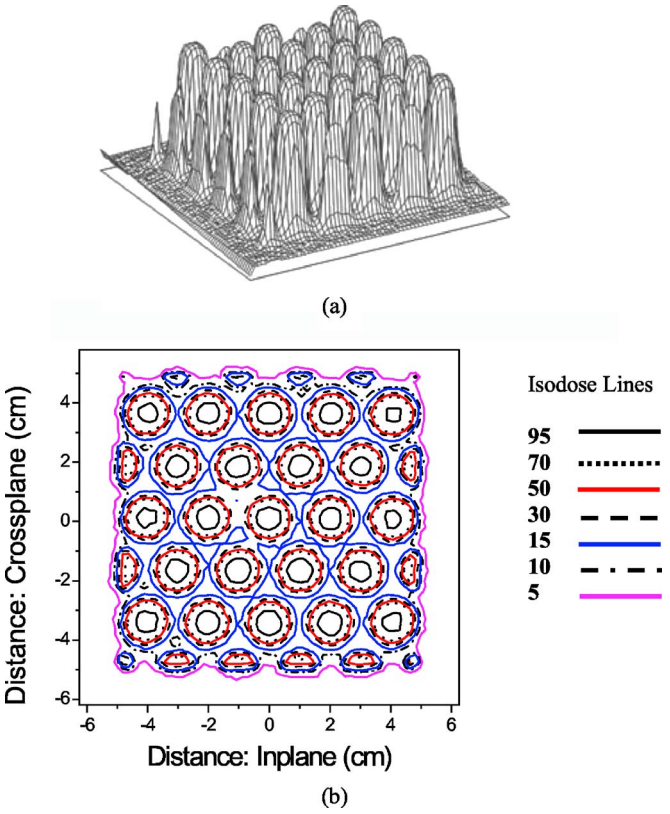

FIG. 7. (a) Dose distribution and (b) isodose curves obtained from 6 MV GRID x-ray irradiation using film dosimetry technique at dmax for a 10 $\times$ 10 cm field size.

at dmax and 100 cm SSD as a function of field size and energy in Table III. These results indicated a good agreement between open field $S_{c,p}$ and GRID output factors for both 6 and 18 MV photon beams.

The cross-plane beam profiles for the newly redesigned GRID block were compared with those of the prototype grid.

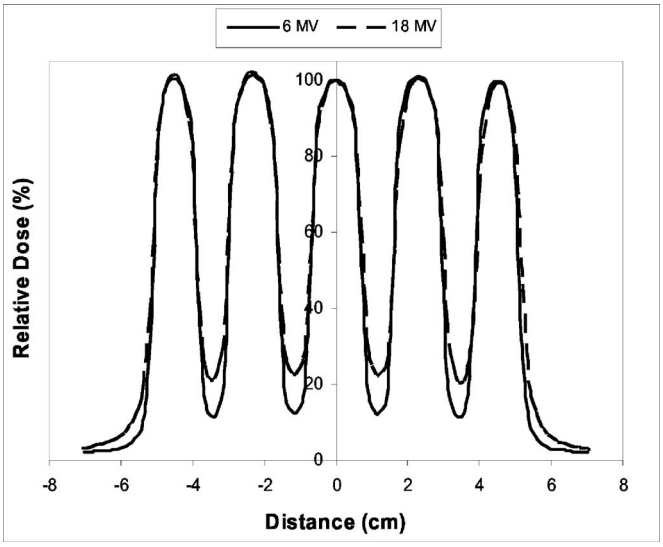

FIG. 8. Comparison of profiles between 6 and 18 MV photons from film dosimetry at the depth of maximum dose at a field size of 10 $\times$ 10 cm.

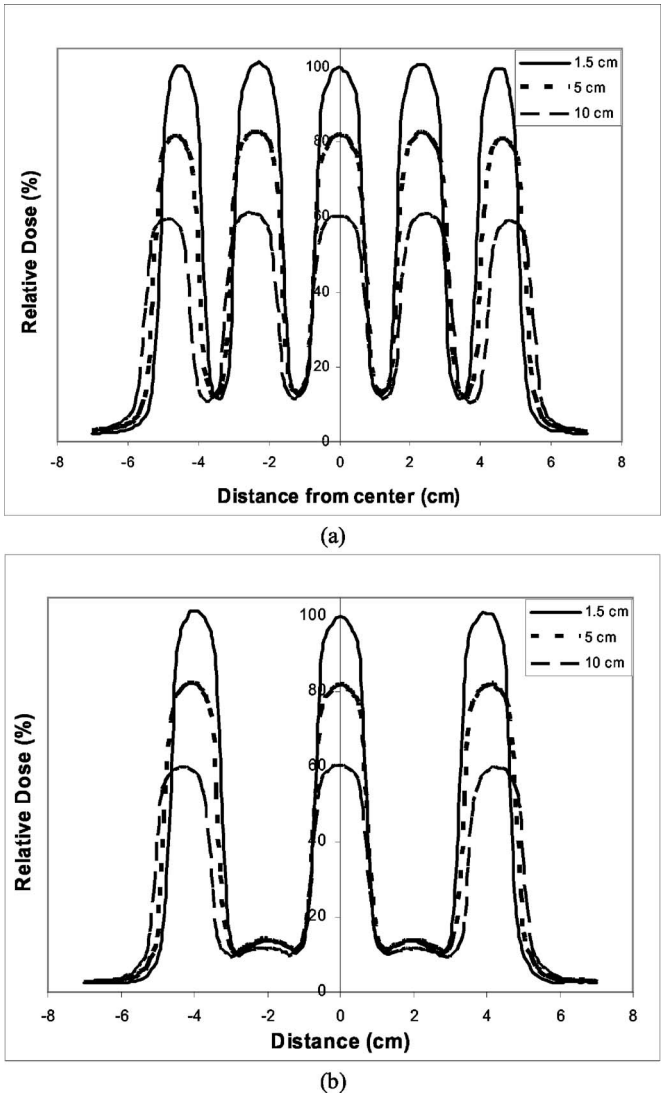

FIG. 9. Depth dependence of (a) cross-plane and (b) in-plane profiles obtained from ionization chamber measurements for 6 MV GRID x-ray beams for a 10 $\times$ 10 cm field size.

These comparisons are shown in Figs. 5(a) and 5(b). These figures show good symmetry and well-patterned dose profiles for both grid designs. However, relative to the prototype grid, the new GRID block shows approximately a 50% dose reduction to the blocked regions of the field for both 6 and 18 MV photons. This reduction can be attributed to the differences of beam divergence and attenuation for the two block designs.

Figures 6(a) and 6(b) show the comparison of measured beam profiles using the film dosimetry technique for an open 10×10 cm^2 field versus GRID field for both 6 and 18 MV photons, respectively. The dose profiles in these figures were normalized to the central axis dose value of the open field. These figures indicate an output factor of 100% for an open field and 90% for a 6-MV GRID field. However, the output factors for 18 MV open and GRID fields were found to be 100% and 78%, respectively. These output factors are utilized for treatment planning of patients treated with GRID.

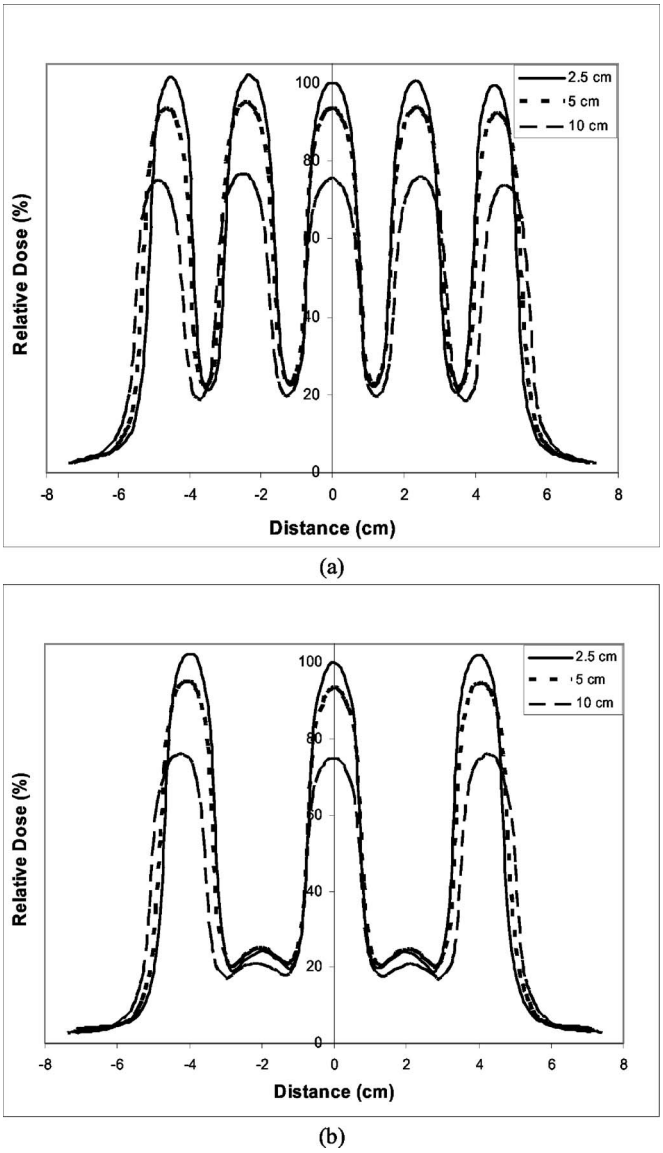

FIG. 10. Depth dependence of (a) cross-plane and (b) in-plane profiles obtained from ionization chamber measurements for 18 MV GRID x-ray beams for a 10×10 cm field size.

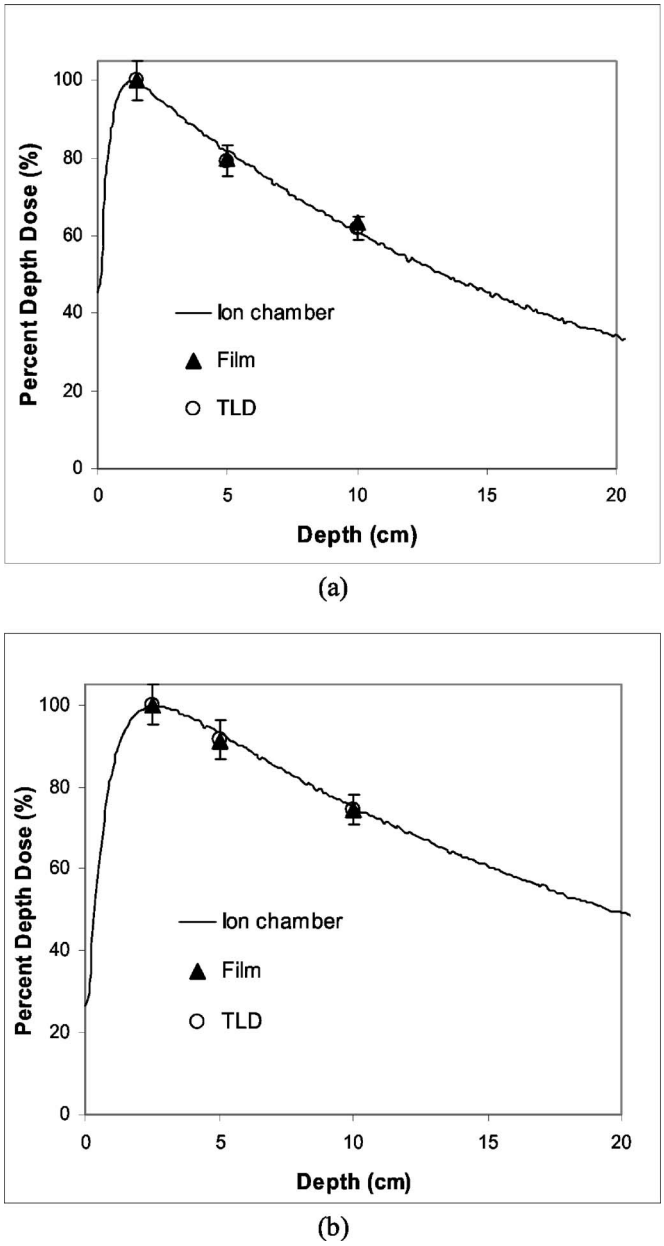

FIG. 11. Percent depth dose (%DD) for a 10×10 cm field along the depth axis of the central aperture for GRID collimated fields of (a) 6 and (b) 18 MV x-ray beams. %DD data were obtained from ionization chamber measurements in water and film and TLD measurements in Solid Water™ phantom material.

Figures 7(a) and 7(b) represent the dose distribution and isodose curves of a GRID radiation field for 6 MV photons, respectively. These figures were obtained using the film dosimetry technique at dmax depth for a 10×10 cm field. Figure 7(b) shows that the minimum contiguous isodose lines between the GRID holes were found to be approximately 12%–16%, which is consistent with TLD and ionization chamber measured data shown in Table I(A). Figure 8 shows a comparison of cross-plane beam profiles for 6 and 18 MV photons at dmax depth for a 10×10 cm field size measured with ionization chamber. This figure indicates similar dose profiles for the two photon energies.

Comparisons of GRID field profiles as a function of depth measured with the film dosimetry technique for 6 and 18 MV photons are shown in Figs. 9 and 10, respectively. Dose profiles at different depths are normalized to the CAX dose at the dmax depth for both beam energies. These figures indicate that the dose to the open region (i.e., hole) of the GRID field decreases with increasing depth, but the dose to the blocked area remains nearly constant. Therefore, the ratio of the peak-to-valley dose decreases with increasing depth.

Figures 11(a) and 11(b) show the %DD of 6 and 18 MV GRID fields, respectively, along the depth axis of the central aperture. These data were measured with an ionization chamber in water, film dosimetry, and TLD in Solid Water™ using a 10×10 cm field size and 100 cm SSD. These results indicate an excellent agreement between the data measured with the three different techniques for both 6 and 18 MV x rays. Figure 12 demonstrates the impact of the field size on the

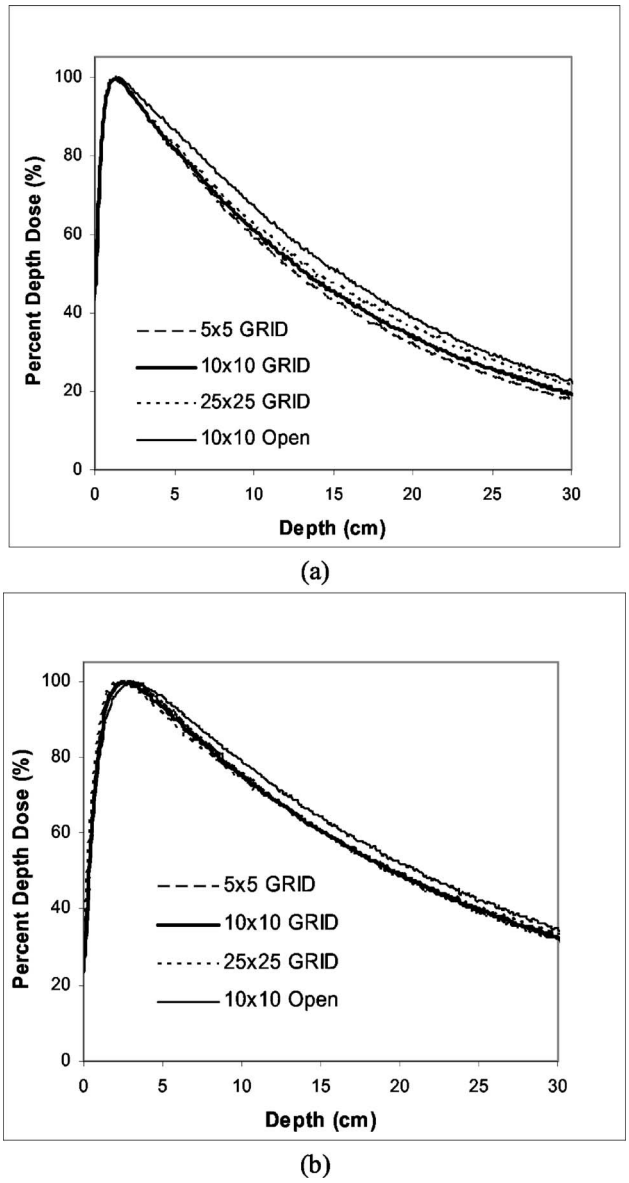

FIG. 12. Percent depth dose (%DD) as a function of field sizes for 6 MV (a) and 18 MV (b) x-ray beams in water phantom.

%DD of 6 and 18 MV beams. As shown in this figure, no significant differences (within ±2.5% at a depth of 30 cm) were observed for the 18-MV beam. However, these differences increase to approximately ±10% for the 6-MV beam at a depth of 30 cm.

B. Cell survival estimation under GRID field irradiation

The surviving fractions of tumor and normal cells are expressed by a linear quadratic model for a single uniform dose irradiation in the linear-quadratic model of cell survival. Typical values for the ratio α/β are 10 Gy for tumor cells and 2.5 Gy for normal tissues.[17,18] If a cell survival of 0.5 for a dose of 2 Gy is assumed, the resulting values of α and β will be 0.289 and 0.0289 for tumor cells and 0.193 and 0.077 for normal tissues. The therapeutic advantage of GRID irradiation was modeled in terms of the normal tissue cell survival ratio of a GRID versus an open field for the same tumor cell kill.[11]

Assuming identical dose distribution under each grid hole (Figs. 9 and 10) at a given depth, the dose profile under the central axis grid hole [Fig. 13(a)] was utilized to calculate the surviving fraction of the cells as a function of absorbed dose following Zwicker *et al.*'s model.[11] Figure 13(b) shows the integral dose area histogram and Fig. 13(c) shows the differential dose area histogram used in these calculations. The cell surviving fraction in tissue irradiated by such a dose distribution is determined and the results were utilized for evaluation of the therapeutic advantage of the GRID with Eq. (2). Figure 14 shows the therapeutic advantage determined for tumor cells with $\alpha=0.289$, $\beta=0.0289$, and $\alpha/\beta=10$, and normal tissue cells with $\alpha=0.193$, $\beta=0.077$, and $\alpha/\beta=2.5$.

IV. CONCLUSIONS

Dosimetric characteristics of a newly redesigned GRID block have been evaluated as a function of field size and beam energy. A dose to the blocked area of the GRID is

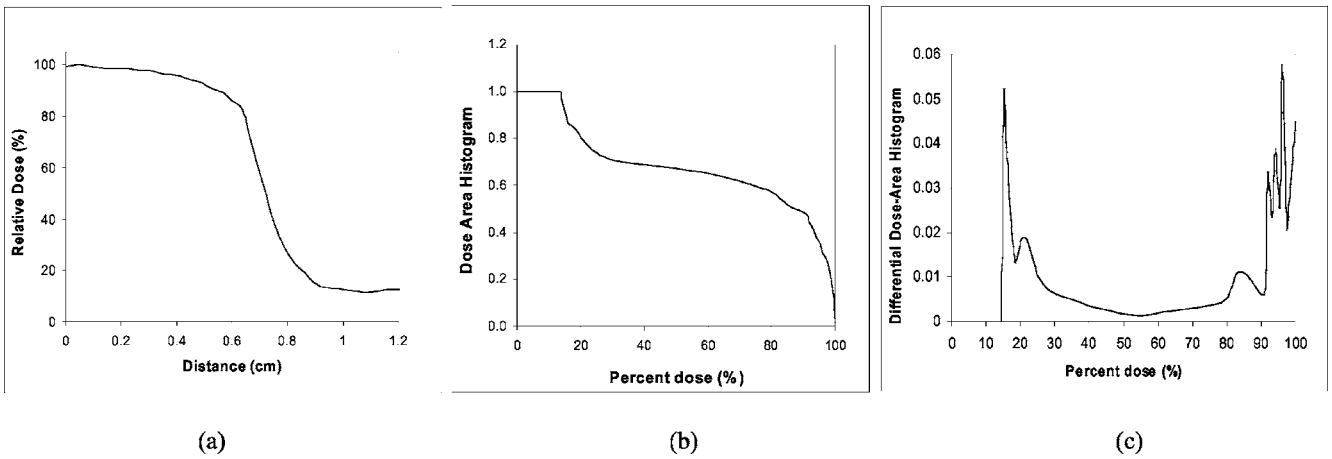

FIG. 13. (a) Representative grid dose profile under one hole, (b) integrated dose area histogram, and (c) differential dose area histogram at dmax for a 6 -MV x-ray beam.

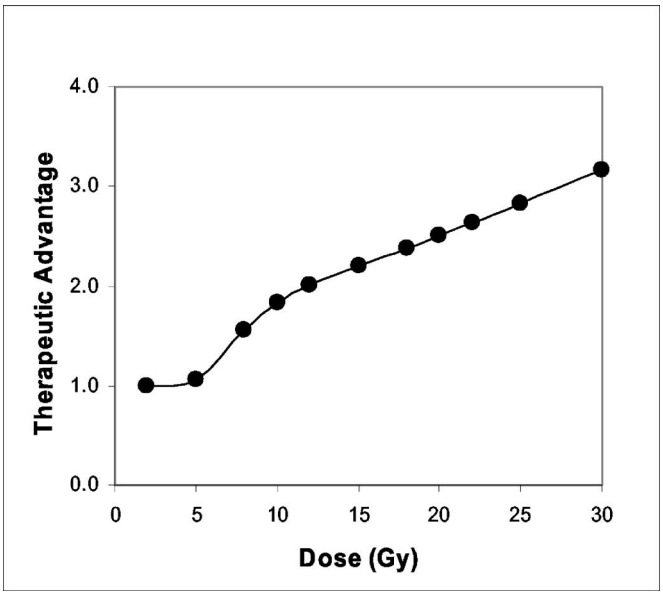

FIG. 14. Calculation of therapeutic advantage of normal cells for a GRID field vs an open uniform field as a function of dose.

significantly reduced compared to that obtained with the prototype grid block. The new GRID shows a large dynamic range of dose across the open and blocked area of the field with the valley-to-peak ratios increasing with increasing beam energy and depth. The field-size-dependent output factors obtained for the GRID are generally consistent with the previously measured open field output factors for this linear accelerator.

The standard linear quadratic model was employed to evaluate this GRID by studying cell survival and therapeutic advantage up to 30 Gy. On the basis of cell survival with a cell survival of 0.5 for a dose of 2 Gy assumed, large single-dose fraction treatment using GRID is expected to have a remarkably therapeutic advantage over open field treatment to achieve the same level of tumor cell killing. A greater therapeutic advantage of 2.20 is, in particular, predicted with GRID therapy at a 15-Gy grid irradiation versus an open field and the therapeutic gain is found to increase with dose. Dosimetric characteristics of a GRID, and corresponding therapeutic advantages of GRID therapy, appear to increase credit in this modality for single high-dose GRID radiotherapy.

ACKNOWLEDGMENTS

The authors would like to thank Dr. Robert Zwicker for valuable discussions.

[a]Author to whom correspondence should be addressed: Ali S. Meigooni, Ph.D., University of Kentucky Medical Center, Department of Radiation Medicine, 800 Rose Street, Lexington, KY, 40536-0084. Tel: (859) 323-6486. Fax: (859) 257-1211. Electronic mail: alimeig@uky.edu

[1]M. Mohiuddin, D. L. Curtis, W. T. Grizos, and L. Komarnicky, "Palliative treatment of advanced cancer using multiple nonconfluent pencil beam radiation: A pilot study," Cancer **66**, 114–118 (1990).

[2]M. Mohiuddin, J. H. Steves, J. E. Reiff, M. S. Huq, and N. Suntharalingam, "Spatially fractionated (GRID) radiation for palliative treatment of advanced cancer," Radiat. Oncol. Invest. **4**, 41–47 (1996).

[3]M. Mohiuddin, M. Fujita, W. F. Regine, A. S. Meigooni, G. S. Ibbott, and M. M. Ahmed, "High-dose spatially fractionated radiation (GRID): A new paradigm in the management of advanced cancers," Int. J. Radiat. Oncol., Biol., Phys. **45**, 721-7 (1999).

[4]M. Mohiuddin, M. Kudrimoti, W. F. Regine, A. S. Meigooni, and R. Zwicker, "Spatially fractionated radiation (SFR) in the management of advanced cancer," Radiother. Oncol. **64** (supplement 1), S313 (2002).

[5]J. E. Reiff, M. S. Hug, M. Mohiuddin, and N. Suntharalingam, "Dosimetric properties of megavoltage grid therapy," Int. J. Radiat. Oncol., Biol., Phys. **33**, 937-42 (1995).

[6]J. V. Trapp, A. P. Warrington, M. Partridge, A. Philps, J. Glees, D. Tait, R. Ahmed, M. O. Leach, and S. Webb, "Measurement of the three-dimensional distribution of radiation dose in grid therapy," Phys. Med. Biol. **49**, N317-23 (2004).

[7]A. S. Meigooni, S. A. Parker, J. Zheng, K. J. Kalbaugh, W. F. Regine, and M. Mohiuddin, "Dosimetric characteristics with spatial fractionation using electron GRID therapy," Med. Dosim **27**, 37–42 (2002).

[8]B. S. Sathishkumar, B. Boyanovsky, A. A. Karakashian, K. Rozenova, N. V. Giltiay, M. Mohiuddin, M. Kudrimoti, M. M. Ahmed, and M. Nikolova-Karakashian, "Elevated sphingomyelinase activity and ceramide concentration in serum of patients undergoing high dose spatially fractionated radiation treatment: Implications for endothelial apoptosis," Cancer Biology and Therapy **4**, 979–986 (2005).

[9]B. S. Sathishkumar, S. Dey, A. S. Meigooni, W. F. Regine, M. Kudrimoti, M. M. Ahmed, and M. Mohiuddin, "The impact of TNF-a induction on therapeutic efficacy following high dose spatially fractionated (GRID) radiation," Technol. Cancer Res. Treat. **1**(2), 141–147 (2002).

[10]A. Niemierko, "Reporting and analyzing dose distribution: A concept of equivalent uniform dose," Med. Phys. **24**, 103–110 (1997).

[11]R. D. Zwicker, A. S. Meigooni, and M. Mohiuddin, "Therapeutic advantage of GRID irradiation for large single fractions," Int. J. Radiat. Oncol., Biol., Phys. **58**, 1309-15 (2004).

[12]A. S. Meigooni, V. Mishra, H. Panth, and J. F. Williamson, "Instrumentation and dosimeter-size artifacts in quantitative thermoluminescence dosimetry of low dose fields," Med. Phys. **22**, 555-61 (1995).

[13]I. Gomola, J. Van Dam, J. Isern-Verdum, J. Verstraete, R. Reymen, A. Dutreix, B. Davis, and D. Huyskens, "External audits of electron beams using mailed TLD dosimetry: preliminary results," Radiother. Oncol. **58**, 163-8 (2001).

[14]A. S. Meigooni, K. Sowards, and M. Soldano, "Dosimetric characteristics of the InterSource ^{103}palladium brachytherapy source," Med. Phys. **27**, 1093–1100 (2000).

[15]P. Karaiskos, A. Angelopoulos, L. Sakelliou, P. Sandilos, C. Antypas, L. Vlachos, and E. Koutsouveli, "Monte Carlo and TLD dosimetry of an ^{192}Ir high dose-rate brachytherapy source," Med. Phys. **25**, 1975-84 (1998).

[16]D. M. Gearheart, A. Drogin, K. Sowards, A. S. Meigooni, and G. S. Ibbott, "Dosimetric characteristics of a new ^{125}I brachytherapy sources," Med. Phys. **27**, 2278–2285 (2000).

[17]D. E. Lee, *Actions of Radiations on Living Cells* (Cambridge University Press, London, 1946).

[18]G. W. Barendsen, "Dose fractionation, dose rate, and isoeffect relationships for normal tissue responses," Int. J. Radiat. Oncol., Biol., Phys. **8**, 1981–1997 (1982).